Chemical Composition and Inhibitory Effect of the Essential Oil from *Mentha Spicata* Irrigated by Wastewater on the Corrosion of Aluminum in 1 Molar Hydrochloric Acid

F. Bensabah,[*] **S. Houbairi, M. Essahli, A. Lamiri and J. Naja**

University Hassan 1, Faculty of Science and Techniques, Laboratory of Applied Chemistry and Environment, B.P. 577, Settat, Morocco

Abstract

Mentha Spicata irrigated by wastewater from the city of Settat (Morocco) was tested as corrosion inhibitor of aluminum in 1 M HCl using polarization method and weight loss measurements. The inhibition efficiency of *mentha spicata* oil was calculated and compared. We note good agreement between these methods. The results obtained showed that the tested inhibitor reduces the kinetic process of corrosion of aluminum.
Its efficiency increases with the concentration and attained 83,01% at 1800 ppm. The effect of temperature on the corrosion behaviour of aluminum in 1M HCl was also studied in the range 283 K and 313 K. The thermodynamic data of activation were determined. The analysis of mentha spicata oil obtained by hydro-distillation using gas chromatography (GC) showed that the major components are carvone 57.11 % and limonene 27.77%.

Keywords: Corrosion inhibition, aluminum, *Mentha Spicata*, essential oil, wastewater.

Introduction

Aluminum and aluminum alloys represent an important category of materials due to their high technological value and wide range of industrial applications, especially in aerospace and house-hold industries [1]. Owing to these applications of aluminum and its alloys, considerable attention has been devoted to the corrosion behaviour of these materials in various aggressive environments [2–3].

---

[*] Corresponding author. E-mail address: bensabah_fati@yahoo.fr

Efforts to stop or delay to the maximum the attack of metals in various corrosive media are made. The use of natural inhibitors may be an alternative to the synthetic inhibitors.

Near their environmental and acceptable ecological properties, naturally occurring antioxidants are cheap and readily available and are renewable sources of materials [4-5]. In this paper, our choice is focused on essential oil of spearmint (*mentha spicata*) in acidic medium.

Mentha spicata (Spearmint) is a creeping rhizomatous, glabrous and perennial herb with a strong aromatic odor. The oil of *mentha spicata* is rich in carvone and presents a characteristic spearmint odor [6]. The species has been found useful as digestive and gastro-stimulant; it is eaten in the form of chutney [7]; leaves are popularly used as tea flavouring agent, while herbalists use the whole plant as carminative [7]. The fresh and dried plants and their essential oils are widely used in food, cosmetic, confectionary, chewing gum, toothpaste and pharmaceutical industries [8]. The essential oil of *mentha spicata* showed strong insecticidal and mutagenic activity [9].

Acidic solutions are used in many industrial areas. The most important applications are acid pickling, industrial acid cleaning, acid descaling, and oil well acidizing [10, 11]. The use of inhibitors is one of the most practical methods for protection against corrosion and prevention of unexpected metal dissolution and acid consumption, especially in acid solutions [12].

Experimental part

Plant material

The planting was made in May 2009 in experimental plots located in the Faculty of Sciences and Technics of Settat-Morocco (FSTS). Irrigation was done with the urban wastewater purified by lagoons from the city of Settat-Morocco. The harvests have been handmade and the plants were cut 15-30 cm above the ground. The quality of essential oils was also determined using fresh leaves of spearmint.

Water quality irrigation

The physico-chemical parameters (temperature, pH and conductivity) were measured on site by means of a mercury thermometer (1/10 °C), a portable pH meter Lutron (pH-206) and a conductivity meter HANNA (HI-8733 with a margin of error of 2%). In the laboratory, the waters were analyzed for major ions (Ca^{2+}, Mg^{2+}, NH_4^+, Cl^-, SO_4^- and HCO_3^-) and the nutritive salts. Chlorides and alkalinity were determined by titration (Appendix Table; Rodier 1996). The analysis of metallic trace elements was carried out by the ICP technique.

Extraction of mentha essential oil

The distillation apparatus consisted of a heating cap, a 1.5 L extraction flask, a cooling system and a receiver for hydrodistillate. Thirty grams of fresh plant leaves and 800 mL of water were used and the distillation was carried out for 3 hours after the mixture reached boiling at 100 °C. Hydrodistillation repetitions were done at least in duplicate depending on the availability of the spearmint leaves. The

essential oil obtained was dried under anhydrous sodium sulfate and stored at 4 °C in the dark before analysis. And the yield of oil derived from the dried leaves was 0.58 %.

Gas chromatography-mass spectrometry

The essential oil was characterized using a gas chromatograph Trace GC Ultra equipped with an auto injector (Triplus) directly interfaced with a mass spectrophotometer with a flame ionization detector (Pdains Q). Capillary column was DB-5 (5% of diphenyl and 95% of dimethylpolysiloxane), 30 m in length, 0.25 mm thickness. Separation conditions were: 25 °C for 2min, 25–200 °C at 4 °C/min, and 180–300 °C at 40 °C/min. Temperature of the injector was 220 °C. The volume injected was 0.1 µL. The carrier gas was helium with a flow rate of 1.4 mL.min^{-1}. The oil constituents were identified by comparison of their retention indices and their mass spectra with those of authentic samples. Quantitative analysis (in percent) was performed by peak area measurement. Table 2 shows the major components of essential oils of spearmint (*mentha spicata*).

Table 1. Characterization of wastewater purified by lagoons used for irrigation.

Parameter	Wastewater purified	
	average value	*Norm*[*]
pH	7,63	6,5-8,4
Temperature /°C	29,36	35
Conductivity at 20 °C µs/cm	1313,64	1200
Biological Oxygen Demand mgO$_2$/L	27	-
Chemical Oxygen Demand mgO2/L	656,36	-
NH$_4^+$ mg/L	11,25	-
Cl$^-$ mg/L	850,7	350
Ca^{2+} mg/L	97,94	-
Mg^{2+} mg/L	53,63	-
HCO$^-_3$ mg/L	67,65	512
N-NO$_2^-$ mg/L	0,09	30
PO$_4^{3-}$ mg/L	3,27	-
SO$_4^{2-}$ mg/L	124,00	350
Suspended matter mg/L	130,4	200
Cd mg/L	≤0.002	0,01
Cr mg/L	0.004	1
Cu mg/L	0,0075	0,2
Ni mg/L	0,012	2
Zn mg/L	0,089	2
Hg mg/L	≤0.01	0,001

(*) : Standards of water quality for irrigation S.E.E.E-2007- Morocco (Secretariat of the Ministry of Energy, Mines, Water and Environment)

Weight loss tests

The aggressive solution (1M HCl) was prepared by dilution of Analytical Grade 37 % HCl with distilled water. Prior to all measurements, the aluminum samples were polished with different emery papers up to 1200 grade, washed thoroughly with distilled water, degreased with acetone and drying at room temperature.

The solution volume was 30 mL. The used aluminum specimens had a rectangular form, with a surface area of 7.5 cm^2. The immersion time for the weight loss was 1 h at 25 °C. After the corrosion test, the specimen of aluminum was carefully washed in distilled water, dried and then weighed. The rinse removed loose segments of the film of the corroded samples. Duplicate experiments were performed in each case and the mean value of the weight loss was reported. Weight loss allowed us to calculate the mean corrosion rate as expressed in mg.cm^{-2} h^{-1}.

Table 2. Chemical composition of the essential oil of *mentha spicata* irrigated by wastewater from the city of Settat (Morocco) purified by lagoon.

Compounds	Retention time	A
α-pinene	8.59	0,69
camphene	9.06	Trace
3-carene	10.04	1,01
β-phellandrene	10.67	0,60
limonene	12.01	27,77
1,8-cineole	14.59	0,28
cis-ocimene	15.88	Trace
borneol	16.85	0,84
sabinene hydrate	17.28	0,39
isocyclocitral	17.94	1,71
trans-carveol	18.87	1,79
pulegone	19.42	0,30
carvone	19.74	57,11
bornyl acetate	21.63	0,27
iso-limonene	22.79	Trace
β-bourbonene	24.32	0,71
caryophyllene	25.12	Absent
aromandrene	25.40	0,50
germacrene D	27.31	0,65
calamenene	27.78	0,22

A: plots irrigated by wastewater from the city of Settat treated lagoon.

Rp, polarisation and EIS measurements

Electrochemical measurements were carried out in a conventional three-electrode electrolysis cylindrical Pyrex glass cell. The working electrode (WE) in the form of disc cut from aluminum has a geometric area of 1 cm^2. A saturated calomel electrode (SCE) and a disc platinum electrode were used respectively as reference and auxiliary electrodes. The temperature was thermostatically

controlled at 25 °C. The WE was abraded with different emery papers up to 1200 grade, degreased with acetone, and rinsed with distilled water before use.

Running on a compatible computer, the Voltab Master4 Software communicates with Instruments potentiostat–galvanostat model PGZ100 at a scan rate of 10 mV/sec. Before recording the polarization curves, the working electrode is maintained for 30 min to Ecorr. The resulting current is plotted as a function of the potential.

Polarization resistance (Rp) values were obtained from the current potential plot. The scan rate was 10 mV/sec.

The electrochemical impedance spectroscopy (EIS) measurements were carried out with an electrochemical system which included a digital potentiostat model Volta lab PGZ 100 computer at Ecorr after immersion in solution, the circular surface of aluminum exposing of 1 cm^2 to the solution was used as working electrode.

Frequencies between 100 kHz and 10 mHz were superimposed on the corrosion potential. The impedance diagrams are given in the Nyquist representation. Values of Rt and C_{dl} were obtained from Nyquist plots.

Results and discussion

Physicochemical analysis of irrigation water

Throughout the experiment, the chemical composition of this water source of irrigation has been determined and is detailed in Table 1. The gravity irrigation planting is done 1 day / 3 sources, and water was analyzed at each irrigation.

Wastewater physico-chemical analyzes showed that the chemical oxygen demand is high and the concentration of Cl$^-$ ion exceeds the standard because urban water is responsible by chloride ions. Other physico-chemical parameters meet the standards as metallic trace elements.

Chemical composition of mentha spicata essential oil

The GC-MS analyzes of *mentha spicata* essential oil irrigated by urban wastewater purified by lagoons from the city of Settat-Morocco are presented in the Table 2.

Mentha spicata of Morocco still contains majority composed: carvone, limonene and trans-carveol. In general, the spearmint oil composition in this study was similar to that in other reports [13, 14, 15].

Weight loss tests

The corrosion rate (W_{corr}) of aluminum in 1M HCl solution at various contents of the natural oil tested was determined after 1 h of immersion period at 25 °C. Values of corrosion rates and inhibition efficiencies are given in Table 3. In the case of the weight loss method, the inhibition efficiency (E_w %) was determined by the following relation:

$$\text{Ew } \% = \frac{W_{corr} - W_{corr(inh)}}{W_{corr}} \times 100 \tag{1}$$

where W_{corr} and $W_{corr(inh)}$ are the corrosion rates of aluminum in the absence and presence of the oil, respectively.

The analysis of these results (Table 3 and Fig. 1) shows clearly that the corrosion rate decreases (W (mg/h.cm^2) while the inhibition efficiency (Ew (%)) increases with increasing inhibitor concentration, reaching a maximum value of 83.01% at a concentration of 1800 ppm. This behaviour can be attributed to the increase of the surface covered θ (Ew % /100) and this is due to the adsorption of natural compounds on the surface of the metal as the inhibitor concentration increases. We can conclude that mentha oil is a good corrosion inhibitor for aluminum in 1M HCl solution.

Table 3. Gravimetric results of aluminum in acid without and with addition of the natural oil at various contents ($t = 1h$. $T = 25\ °C$).

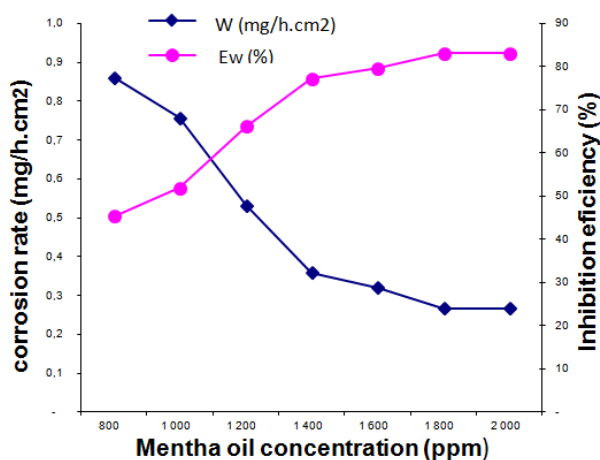| concentration /ppm	W mg/cm^2.h	Ew /%
Blank	1.5740	---
800	0.8610	45.30
1000	0.7566	51.93
1200	0.5328	66.15
1400	0.3592	77.18
1600	0.3205	79.64
1800	0.2674	83.01
2000	0.2674	83.01

Figure 1. Variation of corrosion rate and inhibition efficiency of aluminum in 1M HCl without and with *mentha spicata* oil.

Polarisation measurements

Current-potential characteristics resulting from cathodic polarisation curves of aluminum in molar HCl at various concentrations of the tested mentha oil are evaluated. Fig. 2 shows the typical cathodic Tafel plots of the mentha oil at different concentrations.

Table 4 collects the corrosion kinetic parameters such as E_{corr}, I_{corr} and β_c obtained from potentiodynamic polarization curves for aluminum in 1M HCl containing different concentrations of mentha oil. In the case of polarization method the relation determines the inhibition efficiency (EI %):

$$E_I \% = \frac{Icorr - I\ corr\ (inh)}{Icorr} \times 100 \qquad (2)$$

where I_{corr} and $I_{corr(inh)}$ are the corrosion current density values without and with the inhibitor, respectively, determined by extrapolation of cathodic Tafel lines to the corrosion potential.
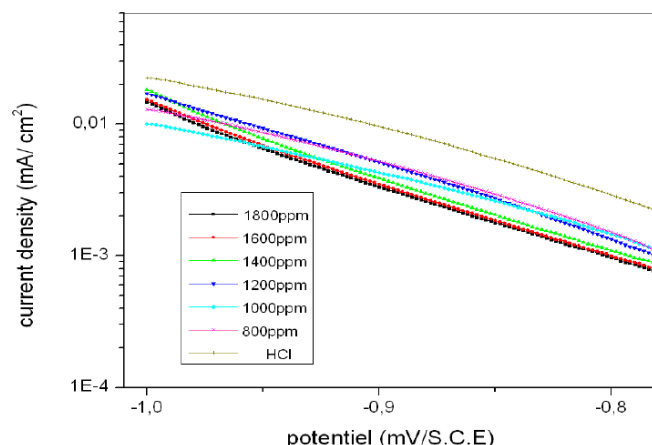

Figure 2. Cathodic plots of aluminum in 1M HCl at various concentrations of *mentha* oil.

Table 4. Electrochemical parameters of aluminum at various concentrations of *mentha* oil studied in 1M HCl at 25 °C. Corresponding corrosion inhibition efficiencies.

inhibitor	concentration ppm	E_{corr} mV/SCE	Icorr mA/Cm^2	βc	Rp	E_I/%
blank	----	-763	2.6693	-249.5	9.20	---
	800	-772.4	1.5367	-241.4	17.42	42.43
	1000	-773.6	1.3948	-262.8	19.83	47.75
	1200	-784.7	0.9446	-285.3	30.70	64.61
mentha oil	1400	-785.5	0.6779	-250.8	42.49	74.60
	1600	-757.4	0.5951	-179.2	38.52	77.70
	1800	-758.6	0.5481	179.4	42.40	79.47
	2000	-758.4	0.5439	183.5	40.06	79.62

From electrochemical polarisation measurements, it is clear that the addition of inhibitor causes a decrease of the current density. The values I_{corr} of aluminum in the inhibited solution are smaller than those for the inhibitor free solution (Table 4). The parallel cathodic tafel plots obtained in Fig.2 indicate that the hydrogen evolution is activation-controlled and the reduction mechanism is not affected by the presence of the inhibitor. The addition of the inhibitor does not change the values of corrosion potential ($_{Ecorr}$) and cathodic tafel slope (βc) when the concentration increases. These results demonstrate that the hydrogen evolution reaction is inhibited and that the inhibition efficiency increases with inhibitor concentration.

In the anodic range (Fig. 3), the polarisation curves of aluminum show that the addition of the natural oil decreases the current densities in large domain of potential. This result suggests that this compound acts as a mixed-type inhibitor.
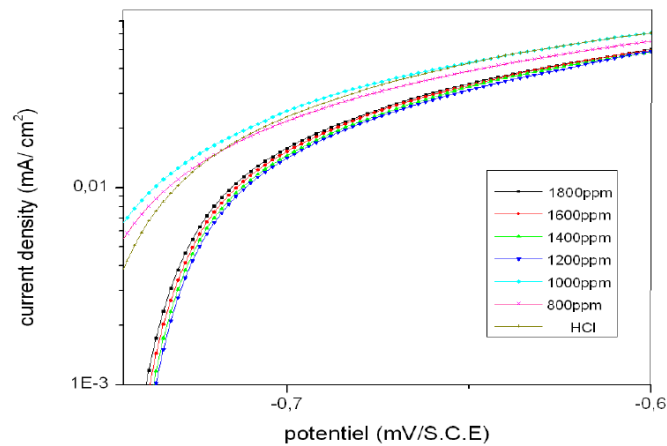
Figure 3. Anodic curves of aluminum in 1M HCl without and with *mentha* oil.

Electrochemical impedance spectroscopy (EIS)

The corrosion behaviour of aluminum in 1M hydrochloric acidic solution, in the absence and presence of mentha oil, is also investigated by electrochemical impedance spectroscopy (EIS) at 25 °C. The charge-transfer resistance (Rt) values are calculated from the difference in impedance at lower and higher frequencies, as suggested by Tsuru et al. [16]. The double layer capacitance (C_{dl}) and the frequency at which the imaginary component of the impedance is maximal (-Zmax) are found as represented in equation:

$$C_{dl} = \frac{1}{Rt}, \text{ where } \omega = 2\pi . f_{max} \qquad (3)$$

Impedance diagrams are obtained for frequency range 100 KHz – 10 mHz for aluminum in 1M HCl in the presence and absence of mentha oil. Nyquist plots for aluminum in 1M HCl and in 1800 ppm concentration of mentha oil are presented in Fig 4.
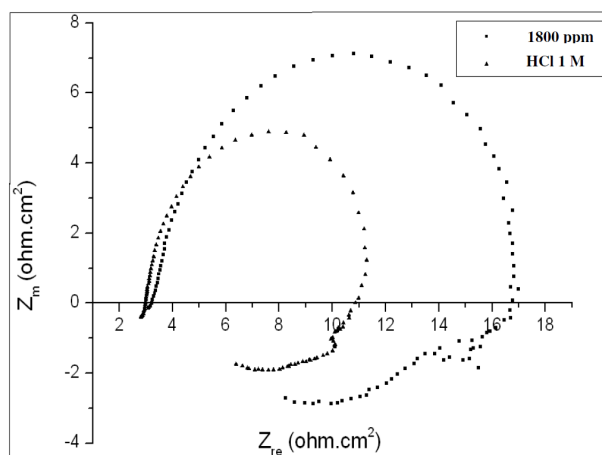

Figure 4. Nyquist plots of aluminum with and without mentha oil.

Table 5 presents values of charge transfer resistance, Rt double-layer capacitance, C_{dl}, and f_{max} derived from Nyquist plots and inhibition efficiency;

the inhibition efficiency gotten from the charge-transfer resistance is calculated by the following relation:

$$E_{Rt}\% = \frac{R't - Rt}{R't} \times 100 \qquad (4)$$

Rt and R't are the charge-transfer resistance values without and with inhibitor, respectively. Rt is the diameter of the loop.

Table 5. Characteristic parameters evaluated from the impedance diagram for aluminum without and with of *mentha* oil.

inhibitor	Rt / (Ohm.cm^2)	f$_{max}$ / Hz	C$_{dl}$ / (µF/cm^2)	E$_{Rt}$/%
blank HCl 1M	36.749	53.55	80.88	--------
mentha oil 1800 ppm	185.207	21.46	40.04	80.15

From the impedance data (Table 5), we conclude that the Rt values increase with inhibitor concentration and consequently the inhibition efficiency increases. As we notice, Fig. 4, the impedance diagrams consist of two capacitive loops. They are not perfect semicircles and this difference has been attributed to dispersion frequency.

The first capacitive loop is wide in high frequency and can be attributed to the charge transfer. The second loop is in an area of low frequencies; it can be attributed to a diffusion phenomenon. [17].

In fact, the presence of mentha oil is accompanied by the increase of the value of Rt in acidic solution indicating a charge transfer process mainly controlling the corrosion of aluminum. Values of double layer capacitance are also brought down to the maximum extent in the presence of the inhibitor. The decrease in C$_{dl}$ is due to the adsorption of the inhibitor on the metal surface leading to the formation of a film or complex from acidic solution [18].

Effect of temperature

The effect of temperature on the corrosion behaviour of aluminum in 1M HCl containing inhibitor at a concentration 1800 ppm is studied in the temperature range 10-40 °C using weight loss measurements. Table 6 regroups the corresponding obtained results.

Table 6. Effect of temperature on the aluminum corrosion in the presence and absence of 1800 ppm oil for 1 hour.

Temperature /°C	W / (mg/cm^2.h)	W'/(mg/cm^2.h)	E/%
10	0.1866	0.0223	88.05
20	0.8803	0.1276	85.51
30	2.2677	0.4556	79.91
40	2.8937	0.6624	77.11

It is obvious that the corrosion rate increases both in the uninhibited and inhibited acid solution with the rise of temperature. The presence of inhibitor leads to the decrease of the corrosion rate, E%, which decreases with the increase of temperature.

The following relation can determine the apparent activation energy:

$$W_{corr} = k \exp (-E_a / RT) \text{ and } W'_{corr} = k' \exp (-E'_a / RT) \qquad (5)$$

W'_{corr} and W_{corr} are the corrosion rates of aluminum with and without inhibitor, respectively. E'_a and E_a are the apparent activation energies in the presence and absence of inhibitor, respectively.
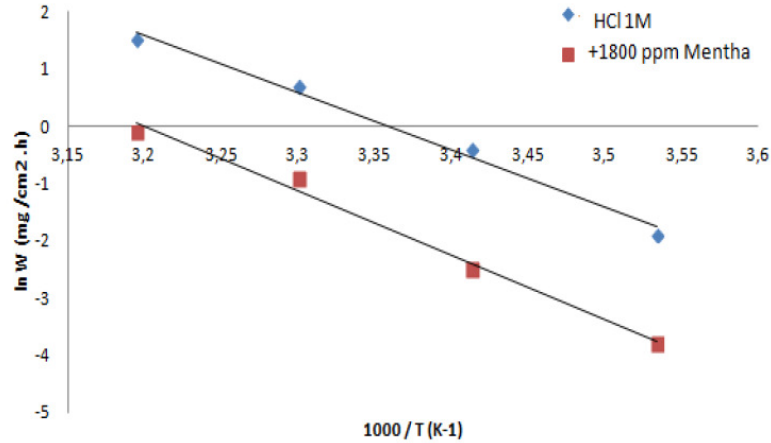

Figure 5. Arrhenius plots of aluminum in uninhibited and inhibited acid.

Arrhenius plots for the corrosion rates of aluminum are shown in Fig. 5. The calculated values of activation energies from the slopes are 83.51 and 93.78 kJ/mol for free acid and with the addition of 1800 ppm of mentha spicata oil, respectively.

Adsorption isotherm
It is found that the activation energy increases in the presence of the inhibitor. Furthermore, the decrease of E% is explained due to the physisorption of the inhibitor molecule on the aluminum surface [21]. The lower value of E_a of the corrosion process in the inhibitors presence when compared to that in its absence is attributed to its chemisorption [19].
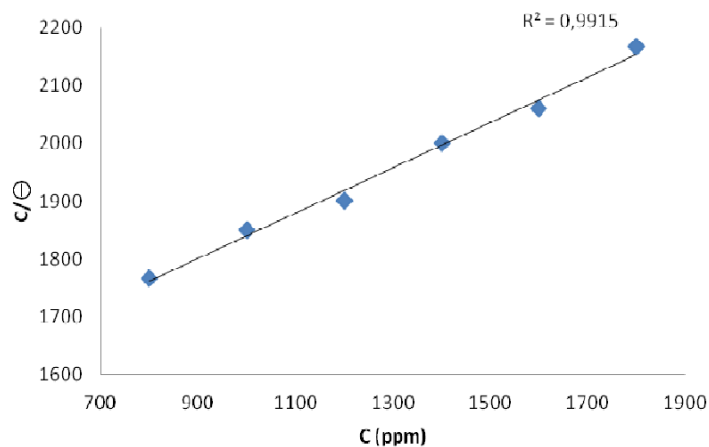

Figure 6. Langmuir adsorption isotherm of mentha oil on the aluminum surface.

The dependence of the fraction of the surface covered Ө obtained by the ratio E%/100 as a function of the oil concentration (C) was graphically fitted for Langmuir, Temkin and Frumkin adsorption isotherms. Fig. 6 shows the

dependence of C/Ө as a function of the oil concentration. The curve obtained clearly shows that the data fit well with Langmuir adsorption isotherm and this was found to be the best description of the adsorption behaviour of the studied inhibitor, which obeys:

$$\frac{C}{\Theta} = \frac{1}{K_{ads}} + C \qquad\qquad (6)$$

C is the inhibitor concentration; Ө is the fraction of the surface covered, K_{ads} is the adsorption coefficient.

The literature shows that the adsorption of heterocyclic compounds occurs with the aromatic rings mostly perpendicular with respect of the metal surface at low concentration, but at elevated inhibitor concentration the molecules are reoriented to the parallel mod [20]. Besides, the adsorption phenomenon may be made by carvone as the principal constituent of the essential oil of *mentha spicata*. But as the natural oil contains so many components, the inhibitory action may also be due to synergistic intermolecular of the active molecules of this oil [21].

Conclusions

From the overall experimental results the following conclusions can be deduced:
- chemical analysis showed carvone as the major component of *mentha spicata* essential oil;
- *mentha spicata* oil acts as good inhibitor for the corrosion of aluminum in HCl medium;
- the inhibition efficiency *of mentha spicata* oil increases with concentration to attain 83% at 1800 ppm;
- the inhibition efficiency of *mentha spicata* oil decreases with the rise of temperature;
- the *mentha essential* oil acts on aluminum surface as mixed inhibitor with a physisorption mechanism.

References
1.   Fouda AS, Al-Sarawy AA, Ahmed FS, et al. Corros Sci. 2009;51:485.
2.   Mercier D, Barthés-Labrousse MG. Corros Sci. 2009;51:339.
3.   Moutarlier V, Gigandet MP, Normand B, et al. Corros Sci 2005;47:937.
4.   El-Etre AY. Corros Sci. 2003;45:2485.
5.   El Hosary AA, Saleh RM, Shams El Din AM. Corros Sci. 1972;12:897.
6.   Jirovetz L, Buchbauer G, Shabi M, et al. Perfum Flav. 2002;27:16.
7.   Yonis YM, Beshir SM. J Essent Oil Res. 2004;16:539.
8.   Lawrence BM. Mint: The Genus Mentha. Boca Raton, FL: CRC Press; 2006.
9.   Franzios G, Mirotsou M, Hatziapostolou E, et al. J Agric Food Chem. 1997;45:2690.

10. Chebabe D, Ait Chikh Z, Hajjaji N. Corros Sci. 2003;45:309.
11. Khaled KF, Hackerman N. Mater Chem Phys. 2003;82:949.
12. Barouni K, Bazzi L, Salghi R, et al. Mater Lett. 2008;62:3325.
13. Znini M, Bouklah M, Majidil L, S. et al. Int J Electrochem Sci. 2011;6:691.
14. El Hassani FZ, Zinedine A, Amraoui MB, et al. Hazardous Materials G Model HAZMAT-9996; No. P7.
15. Bensabah F, A. Lamiri A, Naja J. Eng Sci Tech Int J (ESTIJ). 2013;3.N1.
16. Tsuru T, Haruyama S, Gijutsu B. J Jpn Soc Corros Eng. 1978;27:573.
17. Mansfeld F, Kending MW, Tsai S, Corrosion. 1981;37:301. *ibid.* 1982;38:570.
18. Bentiss F, Lagrenée M, Traisnel M, et al. Corros Sci. 1999;41:789.
19. Dahmani M, Et-Touhami A, Al-Deyab SS, et al. Int J Electrochem Sci. 2010;5:1060.
20. Zarrouk A, Warad I, Hammouti B, et al. Int J Electrochem Sci. 2010;5:1516.